ACS APPLIED MATERIALS & INTERFACES

Research Article

www.acsami.org

Tunable Ultrathin Membranes with Nonvolatile Pore Shape Memory

Hidenori Kuroki,[†] Crescent Islam,[†] Igor Tokarev,[†] Heng Hu,[§] Guojun Liu,[§] and Sergiy Minko*[,†,‡]

[†]Department of Chemistry and Biomolecular Science, Clarkson University, Potsdam, New York 13699, United States

[‡]Nanostructured Materials Lab, University of Georgia, Athens, Georgia 30602, United States

[§]Department of Chemistry, Queen's University, Kingston, Ontario K7L 3N6, Canada

Supporting Information

ABSTRACT: The concept of a responsive nanoporous thin-film gel membranes whose pores could be tuned to a desired size by a specific "molecular signal" and whose pore geometry becomes "memorized" by the gel is reported. The ~100 nm thick membranes were prepared by dip-coating from a solution mixture of a random copolymer comprising responsive and photo-cross-linkable units and monodisperse latex nanoparticles used as a sacrificial colloidal template. After stabilization of the films by photo-cross-linking the latex template was removed, yielding nanoporous structures with a narrow pore size distribution and a high porosity. The thin-film membranes could be transferred onto porous supports to serve as tunable size-selective barriers in various colloids separation applications. The pore dimensions and hence the membrane's colloidal-particle-size cutoff were reversibly regulated by swelling–shrinking of the polymer network with a specially selected low-molar-mass compound. The attained pore shape was "memorized" in aqueous media and "erased" by treatment in special solvents reverting the membrane to the original state.

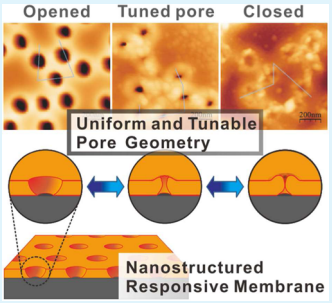

KEYWORDS: *nanostructure, responsive membrane, pore memory, template, size-selective filtration*

INTRODUCTION

Stimuli-responsive membranes,[1−3] which exhibit changes in the pore geometry in response to external stimuli, such as temperature,[4−9] pH,[10−13] light,[14] magnetic field,[15] oxidation–reduction state,[16,17] specific ions,[18,19] chemical reagents,[20,21] or proteins,[22,23] can regulate the transport of small molecules, particles, proteins, viruses, and cells via the pore gating triggered by the stimuli. Most of the stimuli-responsive membranes have been prepared via grafting of responsive polymers on pore walls of multimicrometer-thick filtration membranes. The relatively thick selective layers of such membranes possess a high hydrodynamic resistance. Recently, a number of studies have focused on the development of stimuli-responsive membranes using various thin (typically, less than 1 μm) porous platforms[24] prepared by lithography techniques,[25−27] focused ion beam etching,[28] phase-separation of block copolymer thin films,[29−36] and templating with colloidal particles,[37−39] cross-linked nanoparticles[40] or proteins.[41] Such thin membranes have a much lower hydrodynamic resistance and small cross-sectional dimensions appropriate for various applications from membrane-based separation technologies to miniaturized devices. In our previous publications, we have demonstrated responsive gel thin-film membranes (in a thickness range of 100–200 nm) with two–dimensionally arranged pores using simple phase separation methods.[42−45] Their pore size can be varied in the range of 200 nm to 1 μm at the open state. Furthermore, the pore geometry (size and shape) of the responsive membranes can be tuned by applying external stimuli (e.g., pH change and interactions with specially selected low-molecular-weight substances), due to swelling and shrinking of the entire membrane. The dynamically changeable pore–geometries provide a unique opportunity for the regulation of mass transport through the membrane, thus, enabling design of novel smart systems for various applications, such as flow control, size–selective filtration, chemical and biological separations, controlled release of chemical substances and drugs, chemical sensors, and biosensors.

In addition to the smart dynamic systems whose pore geometries are sensitive to the changeable membrane's environment, another property of stimuli-responsive membranes valuable for practical applications would be the ability to adjust and then stiffen the demanded pore geometry. The pore size adjustment could be conducted in the first step by changing the membrane environment. Then, the membrane could be "frozen" at the desired state in the second step. The porous membrane of this kind could be used as a universal platform for various applications when the pore size could be adjusted and memorized by the membrane. This membrane property is named here *nonvolatile pore shape memory*. A method for the stabilization of pore geometry of porous films with adjustable nonvolatile pore shape memory, introduced in this article, is demonstrated using a colloidal template membrane as an example. However, the introduced concept could be applied for membranes prepared using different fabrication methods when the pores are adjusted and stabilized

Received: February 18, 2015
Accepted: April 26, 2015
Published: April 27, 2015

DOI: 10.1021/acsami.5b01416
ACS Appl. Mater. Interfaces 2015, 7, 10401−10406

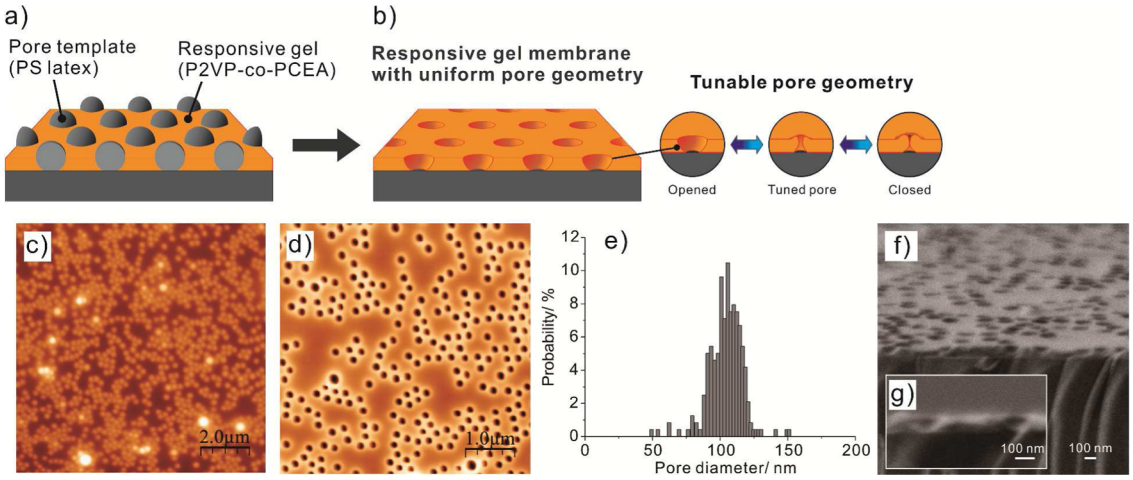

Figure 1. Schematic (a and b) and corresponding AFM topological images (c and d) of the nanostructured P(2VP-co-CEA) gel membrane, prepared by the template method: (a and c) The gel film with embedded PS latex particles on the substrate. (b and d) The gel membrane with uniform pore sizes formed after dissolution of the latex template. (e) The pore size distribution estimated from the AFM image (d). (f) Cross-sectional SEM image of the membrane (after removal of the latex template and prior to plasma treatment) with a zoomed-in area (g).

with a reversible physically cross-linked network that provides pore shape memory.

EXPERIMENTAL SECTION

The nanoporous responsive gel membranes were fabricated via a colloidal template method. A copolymer of P(2VP-*co*-CEA) (P2VP:PCEA = 80:20 mol %, M_n = 68,000 g mol^{-1}, M_w/M_n = 1.8), which was synthesized using the free radical polymerization (see the Supporting Information for details), and 210 nm monodisperse polystyrene (PS) latex particles from Invitrogen life technologies were used. A 4 wt % aqueous dispersion of PS latex nanoparticles (pH 5.5) was added dropwise to an 8 wt % P(2VP-*co*-CEA) solution (pH 2.0) while sonicating until a volume ratio of 1:1 was reached. After additional sonication for 30 min, the mixture was deposited by dip-coating on Si or glass substrates under low humidity (<10% RH). Prior to dip-coating, the clean substrates were immersed in a 0.3 wt % aqueous solution of poly(diallyldimethylammonium chloride) (PDDA, Aldrich) for 15 min and washed with DI water three times. The thickness of the PDDA layer was about 0.3 nm as measured with ellipsometry (Multiskop null-ellipsometer, Optrel). The positively charged PDDA adsorption layer aided the deposition of negatively charged latex particles via electrostatic interactions. The obtained copolymer films with embedded PS nanoparticles were photo-cross-linked by UV irradiation for 30 min. A 100 W mercury lamp equipped with a 280 nm cut−off filter was used as a UV source. Afterward, the films were treated with plasma to etch away an ultrathin P2VP layer covering the PS latex particles. The plasma etching was performed for 5 min at the air pressure of 600 mTorr and the power of ∼10W using a benchtop plasma cleaner (Harrick Plasma). Finally, the films were immersed in toluene and subsequently in chloroform for 30 min in each solvent to dissolve the PS latex template. This was followed by additional plasma treatment for 5 min to remove any residual polymer at the pore bottom.

The nanostructured surfaces of the resulting porous membranes were examined in the dry state using atomic force microscopy (AFM, Dimension 3100 Scanning Probe Microscope, Vecco Instruments, and Multimode 8, Bruker). The membrane's thickness was determined using an AFM "scratch test". In this procedure, a sharp steel needle was used to scratch the membranes down to the surface of the silicon substrate, producing a step with a height equal to the membrane thickness (note that the needle does not damage the harder substrate surface, and the thickness of the PDDA layer was negligible). The AFM images were processed using WSxM[46] and Gwyddion[47] software.

Cross−sectional views of the membrane were obtained by fracturing a membrane-coated thin glass slide in liquid N_2, with the subsequent visualization of fractured regions using a high resolution field emission scanning electron microscope (FE-SEM, JSM-7400, JEOL).

The gold nanoparticles (AuNPs) with positively−charged surfaces were synthesized by the previously reported method.[48] The particle size was found to be 32 ± 7 nm by the AFM analysis of a monolayer of the particles adsorbed onto a Si substrate. For the demonstration of nanoparticle transport through the pores, the membranes were immersed in the AuNP solution at pH 7.2 for 3 h, and then washed with DI water (pH 5.5) five times. The resulting membranes were dried in a N_2 gas flow and analyzed with AFM to identify the locations of adsorbed AuNPs.

RESULTS AND DISCUSSION

Fabrication of porous gel membranes. The method of the membrane's preparation (Figure 1a,b) employs a colloidal template and is briefly summarized below. First, the films were deposited on solid substrates by dip−coating of aqueous solutions of a vinylpyridine copolymer blended with monodisperse latex nanoparticles. The random copolymer comprising responsive 2-vinylpyridine and photo-cross-linkable 2−cinnamoylethyl acrylate units (P(2VP-*co*-CEA)) and monodisperse 210 nm PS latex particles were used. The solid substrates were treated with positively charged PDDA before the deposition; the adsorbed ca. 0.3 nm thick PDDA layer allowed negatively charged PS latex particles to efficiently adsorb on the substrates through electrostatic interactions. The prepared films were photo-cross-linked, and afterward plasma−treatment was conducted to remove an ultrathin P2VP layer that remained on top of the PS nanoparticle template. Finally, dissolution of the latex particles in a selective solvent resulted in the formation of porous gel membranes with a narrow pore size distribution that mirrors a low polydispersity of the latex template. The resulting membrane thickness was found to be 95 ± 15 nm.

The AFM topological image of the film with embedded latex particles (Figure 1c) shows a random particle distribution on the surface; the nanoparticle's clustering was observed in a very small area of the surface. After dissolution of the latex particles, a uniform porous structure was obtained without visible defects (such as two or more merged pores, Figure 1d). The estimated pore diameter of the membrane was 105 ± 13 nm (as measured at the half height of the pore depth; obviously the measured

DOI: 10.1021/acsami.5b01416
ACS Appl. Mater. Interfaces 2015, 7, 10401−10406

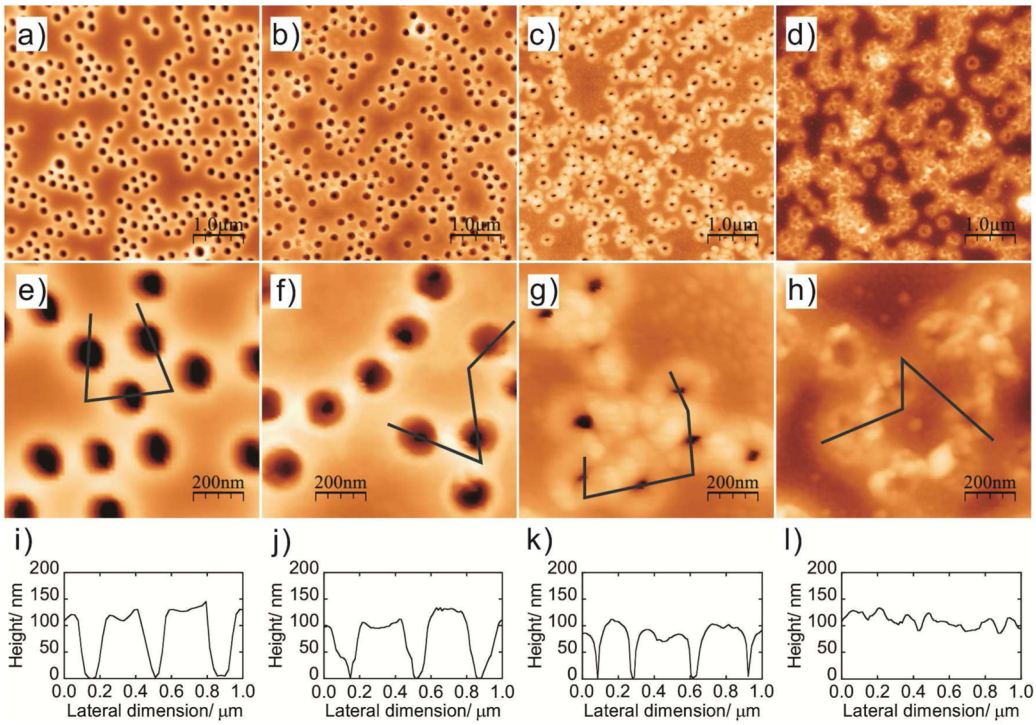

Figure 2. AFM topological images of the responsive gel membranes loaded with PDP from solutions of the following concentrations: (a, e, i) 0, (b, f, j) 13, (c, g, k) 26, and (d, h, l) 130 mM. The image sizes of (a–d) and (e–h) are $5 \times 5\ \mu m^2$, and $1 \times 1\ \mu m^2$, respectively. The cross-sectional profiles (i–l) are obtained along the lines shown in the images (e–h).

pore size in this case is smaller than that of the colloid template), implying a great pore-size distribution control (Figure 1e). Indeed, in the cross-sectional images of the membrane in Figure 1f and 1g, the hemispherical shape of the pores was observed; it is originated from the spherical shape of the latex particles as a pore template. The membranes' pore density was 10^9 pores cm^{-2} which is within the range of pore densities of two types of commercial filtration membranes, having comparable pore-size distributions and pore diameters: polymeric track-etch membranes and anodized aluminum oxide (AAO) membranes.[24] Although it is hard to attain a very dense pore structure with the latex template method, it was chosen for its ease of creating nearly monodisperse pores of desired dimensions in thin films when changes in pore size can be monitored using conventional methods such as SEM and AFM.

The thickness of the prepared membranes was about 100 nm, which should permit fast transport rates through open pores in filtration applications. Obviously, these membranes cannot operate as stand-alone filters for separation. Such delicate nanolayers have to be immobilized on robust high-permeable porous supports. In this implementation, they are reminiscent of broadly commercially available polymeric membranes prepared by phase inversion methods, whose asymmetric pore geometry implies that the pore sizes becomes small in a thin layer on one of the membrane sides. This so-called "skin" layer dominates the overall filtration properties of the membrane, whereas the rest of the material with a larger, more open pore structure acts as a mechanically robust support. Unlike the phase-inversion membranes, which are formed in a single phase separation process and hence offer a very limited control over a pore structure in the filtration skin layers, the fabrication of the skin layers and supports in our approach is decoupled, thus enabling a much greater control over a pore size distribution. On the other hand, the approach, in which the skin and support are made in separate processes, requires the development of methods of integration of both materials into a robust hybrid structure suitable for practical applications. Such integration can be achieved either by transferring an existing skin layer onto a suitable porous support or by direct preparation of this layer on the support. In this study, we transferred the skin layers onto porous supports, specifically on top of 200-nm-pore-size, 60-μm-thick AAO filtration membranes (see the Supporting Information for details). The transferred porous films were chemically bonded to the AAO supports to avoid their delamination during mass transport experiment. The water permeability of the resulting hybrid membranes was found to be $\sim 10^{-8}$ $m^3/(m^2\ s\ Pa)$, which is similar to the previously reported block copolymer asymmetric membranes with the ~100 nm thick skin layer.[49] This value is close to the estimated value of an original AAO support using Hagen–Poiseuille equation. It implies that the ~100 nm thin skin layer causes a little resistance to water permeation. The low membrane's thickness ensured a high flux even at a low applied pressure.

Pore size adjustment and memorizing. Strong binding of 3-pentadecyl phenol (PDP) to P2VP via hydrogen bonds[50,51] was used to regulate and adjust the pore diameter. PDP loading into the P2VP network was carried out from chloroform—a good solvent for both components. The membranes were exposed to PDP solutions of different concentrations for 10 min, and then they were rinsed with *n*-hexane to remove the excess of PDP from the membrane surfaces; *n*-hexane is a good solvent for PDP, whereas it is a nonsolvent for P2VP, thereby enabling selective removal of PDP that did not penetrate inside the P2VP network. The AFM images of the responsive membranes before and after PDP binding are shown in Figure 2a–d. The average size of the open pores at the half and quarter of the pore length (as

DOI: 10.1021/acsami.5b01416
ACS Appl. Mater. Interfaces 2015, 7, 10401–10406

measured from the substrate) was estimated from the AFM images and summarized in Table 1. A decrease in the pore size was observed after the PDP binding into the P2VP network. When the PDP concentration was increased to 26 mM, the pore dimensions at both the 1/2 and 1/4 pore length were found to become profoundly smaller (about 40—50 nm in diameter). The buckling around the pores is also apparent, indicating the swelling-induced mechanical stress in the polymeric network.[52] After the treatment with the 13 mM and 26 mM PDP solutions, the pore-size distribution became broader compared to the initial state of the membrane, and a small fraction of pores turned to be closed. This can be explained by initial variation on the pore sizes and some differences in the cross-linking degree throughout the P2VP network. Eventually, all the pores became completely closed due to the binding of 130 mM PDP inside the membrane, which was accompanied by the strong buckling around the pores. Interestingly, most network deformation occurred in the lateral dimension, whereas the membrane thickness underwent a little change after the PDP binding, remaining close to 100 nm. The presented results demonstrate a fine control over the pore size and porosity, as well as the ability to switch the membrane's pores between the open and closed states (a valve function). Unlike other known responsive membranes,[1−3,42−45] the adjusted pore dimensions are stabilized by strong binding of PDP to P2VP. PDP is not soluble in water. Thus, the PDP-tuned membranes, when used for filtration of aqueous solutions, will preserve their preset pore size due to the mechanism of nonvolatile pore shape memory.

Table 1. Geometrical Properties of the Nanostructured Responsive Gel Membranes

PDP conc (mm)	Pore diameter[a] (nm)	Pore diameter[b] (nm)	Pore density[c] (pores cm^{-2})
0	105 ± 13	83 ± 13	1×10^9
13	102 ± 20	62 ± 22	9×10^8
26	48 ± 18	42 ± 17	7×10^8
130	0	0	0

[a,b]Estimated at the half and quarter of the pore length (as measured from the membrane bottom), respectively. [c]The number of opened pores counted at the quarter of the pore length.

As shown above, the membrane swelling caused nonuniform contraction of the pores along their radial axes. Such unique changes to the pore geometry, leading to the formation of a narrow (bottleneck) region close to the substrate, are likely a consequence of the initial half−round shape of the pores. It is noteworthy, that the pore geometries of the PDP-loaded membranes returned to the initial state by washing PDP off the membranes in chloroform (but not water), and thus, the membrane's response to PDP was reversible (see the Supporting Information). Since the pore geometry of the developed responsive membranes can be repeatedly altered by a molecular signal, a single responsive membrane could be fine-tuned to achieve a desired pore size in a range from 0 to about 100 nm, while preserving a relatively narrow pore size distribution.

Size discrimination by tunable pores. The demonstrated property of precise tuning of the pore sizes provides the opportunity to create a universal membrane that could be adapted for gating the transport of nanoparticles, macromolecules, and proteins through the pores. To demonstrate the ability of the membranes to discriminate colloids by their size, we carried out a simple experiment in which charged inorganic nanoparticles were prompted to adsorb onto an oppositely charged solid substrate overcoated with a P2VP membrane that acted as a size-selective barrier for the particles. Coupled with AFM visualization, it provided us with visual clues on the discriminating properties of the membranes. Briefly, membrane samples with the pore diameter of about 110—130 nm (measured at the quarter height) and the thickness of ca. 100 nm were prepared on Si substrates and exposed to PDP solutions of different concentrations (26 mM and 130 mM). Afterward, the membranes were immersed into dispersion of 32 nm positively−charged gold nanoparticles (AuNPs). The positive charge reduced adsorption of the particles on the membrane surface, while favoring their adsorption onto the negatively charged Si substrate accessible through the open pores. The AFM images after immersing the membranes in an aqueous dispersion of AuNPs (pH 7.2) are shown in Figure 3a−c. The nanoparticles were found to reside at the bottom of

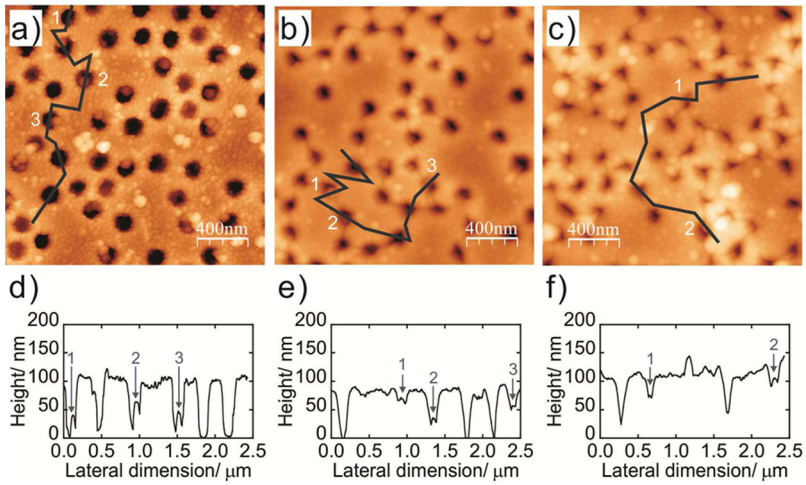

Figure 3. AFM topological images of the PDP-loaded responsive membranes after the adsorption of AuNPs. The different concentrations of PDP were employed for the tuning of the pore size: 0 (a), 26 (b), and 130 mM (c). The size of the images (a−c) is 2×2 μm^2. The cross-sectional profiles (d−f) are obtained along the lines shown in the images (a−c).

DOI: 10.1021/acsami.5b01416
ACS Appl. Mater. Interfaces 2015, 7, 10401−10406

the nontreated membrane, which indicates that the membrane's open pores are large enough for the nanoparticles to pass the pores. In the case of 26 mM PDP, the average pore size (34 ± 15 nm) became close to the nanoparticle diameter. The AFM data in Figure 3b,e show that most of the nanoparticles were trapped in the middle of the pores, or adsorbed on the membrane surface. However, a few nanoparticles, which reached the pore bottom, were also identified. Therefore, the access of the nanoparticles to the substrate was largely blocked. As the PDP concentration increased to 130 mM, the pores became closed, and the transport of the particles was completely barred (Figure 3c,f).

Our experiments show that the swollen membrane's morphology formed due to the PDP binding was preserved after immersing in a phosphate buffer solution at pH 7.2 for 3 h because of the insolubility of PDP in water. In the previously reported responsive membranes, the changes in external media (temperature, pH, ionic strength, etc.) were used to achieve pore gating properties. However, especially in biological applications, a range of operating conditions is typically very limited because of the delicate nature of biomolecules, viruses, and cells. Therefore, the nonvolatile pore shape memory in phosphate buffers provides a great advantage in the biological and biomedical fields.

CONCLUSIONS

We developed here the concept of nanoporous responsive thin membranes with nonvolatile pore shape memory when the responsive membranes possess tunable pore geometry via the swelling−shrinking of the membrane's polymer network triggered by the specially selected "molecular signal", and the pore geometry could be memorized by the membrane stiffening. The membranes can be adjusted to a desired pore size in the range from 0 to about 100 nm, while maintaining a relatively narrow pore size distribution. The pore memory effect could be "deleted" by treatment in special solvents. The membranes have a small thickness and a high pore density, resulting in high permeability. The P2VP membrane platform could be decorated with grafted hydrophilic polymers to exhibit long-lasting antifouling surfaces.[53]

ASSOCIATED CONTENT

Supporting Information

Detailed procedures for the synthesis of a random copolymer, the preparation of porous thin-film membranes, the transfer of the membranes onto porous supports, results of water filtration tests and tuning of the pore geometry. The Supporting Information is available free of charge on the ACS Publications website at DOI: 10.1021/acsami.5b01416.

AUTHOR INFORMATION

Corresponding Author

*E-mail: sminko@uga.edu.

Notes

The authors declare no competing financial interest.

ACKNOWLEDGMENTS

H. Kuroki thanks the Japan Society for the Promotion of Science (JSPS, Japan) for the support of his research fellowship. We acknowledge the support of NSF award DMR-1107786. We also thank Ted Champagne (Instrumentation Technician, Clarkson University) for his assistance with the FE-SEM measurements.

REFERENCES

(1) Ulbricht, M. Advanced Functional Polymer Membranes. *Polymer* **2006**, *47*, 2217−2262.
(2) Tokarev, I.; Minko, S. Stimuli-Responsive Porous Hydrogels at Interfaces for Molecular Filtration, Separation, Controlled Release, and Gating in Capsules and Membranes. *Adv. Mater.* **2010**, *22*, 3446−3462.
(3) Kuroki, H.; Tokarev, I.; Minko, S. Responsive Surfaces for Life Science Applications. *Annu. Rev. Mater. Res.* **2012**, *42*, 343−372.
(4) Park, Y. S.; Ito, Y.; Imanishi, Y. Permeation Control through Porous Membranes Immobilized with Thermosensitive Polymer. *Langmuir* **1998**, *14*, 910−914.
(5) Chu, L. Y.; Li, Y.; Zhu, J. H.; Chen, W. M. Negatively Thermoresponsive Membranes with Functional Gates Driven by Zipper-Type Hydrogen-Bonding Interactions. *Angew. Chem., Int. Ed.* **2005**, *44*, 2124−2127.
(6) Lokuge, I.; Wang, X.; Bohn, P. W. Temperature-Controlled Flow Switching in Nanocapillary Array Membranes Mediated by Poly(N-isopropylacrylamide) Polymer Brushes Grafted by Atom Transfer Radical Polymerization. *Langmuir* **2007**, *23*, 305−311.
(7) Kuroki, H.; Ohashi, H.; Ito, T.; Tamaki, T.; Yamaguchi, T. Isolation and Analysis of a Grafted Polymer onto a Straight Cylindrical Pore in a Thermal-Responsive Gating Membrane and Elucidation of Its Permeation Behavior. *J. Membr. Sci.* **2010**, *352*, 22−31.
(8) Tomicki, F.; Krix, D.; Nienhaus, H.; Ulbricht, M. Stimuli−Responsive Track-Etched Membranes via Surface-Initiated Controlled Radical Polymerization: Influence of Grafting Density and Pore Size. *J. Membr. Sci.* **2011**, *377*, 124−133.
(9) Frost, S.; Ulbricht, M. Thermoresponsive Ultrafiltration Membranes for the Switchable Permeation and Fractionation of Nanoparticles. *J. Membr. Sci.* **2013**, *448*, 1−11.
(10) Mika, A. M.; Childs, R. F.; Dickson, J. M.; McCarry, B. E.; Gagnon, D. R. A New Class of Polyelectrolyte-Filled Microfiltration Membranes with Environmentally Controlled Porosity. *J. Membr. Sci.* **1995**, *108*, 37−56.
(11) Liu, G.; Lu, Z.; Duncan, S. Porous Membranes of Polysulfone-*graft*-poly(*tert*-butyl acrylate) and Polysulfone-*graft*-poly(acrylic acid): Morphology, pH-Gated Water Flow, Size Selectivity, and Ion Selectivity. *Macromolecules* **2004**, *37*, 4218−4226.
(12) Lee, D.; Nolte, A. J.; Kunz, A. L.; Rubner, M. F.; Cohen, R. E. pH-Induced Hysteretic Gating of Track-Etched Polycarbonate Membranes: Swelling/Deswelling Behavior of Polyelectrolyte Multilayers in Confined Geometry. *J. Am. Chem. Soc.* **2006**, *128*, 8521−8529.
(13) Cho, Y.; Lim, J.; Char, K. Layer-by-Layer Assembled Stimuli-Responsive Nanoporous Membranes. *Soft Matter* **2012**, *8*, 10271−10278.
(14) Park, Y. S.; Ito, Y.; Imanishi, Y. Photocontrolled Gating by Polymer Brushes Grafted on Porous Glass Filter. *Macromolecules* **1998**, *31*, 2606−2610.
(15) Yang, Q.; Himstedt, H. H.; Ulbricht, M.; Qian, X.; Wickramasinghe, S. R. Designing Magnetic Field Responsive Nanofiltration Membranes. *J. Membr. Sci.* **2013**, *430*, 70−78.
(16) Ito, Y.; Nishi, S.; Park, Y. S.; Imanishi, Y. Oxidoreduction-Sensitive Control of Water Permeation through a Polymer Brushes-Grafted Porous Membrane. *Macromolecules* **1997**, *30*, 5856−5859.
(17) Jeon, G.; Yang, S. Y.; Byun, J.; Kim, J. K. Electrically Actuatable Smart Nanoporous Membrane for Pulsatile Drug Release. *Nano Lett.* **2011**, *11*, 1284−1288.
(18) Ito, T.; Hioki, T.; Yamaguchi, T.; Shinbo, T.; Nakao, S.; Kimura, S. Development of a Molecular Recognition Ion Gating Membrane and Estimation of Its Pore Size Control. *J. Am. Chem. Soc.* **2002**, *124*, 7840−7846.
(19) Liu, Z.; Luo, F.; Ju, X.-J.; Xie, R.; Luo, T.; Sun, Y.-M.; Chu, L.-Y. Positively K^+-Responsive Membranes with Functional Gates Driven by

DOI: 10.1021/acsami.5b01416
ACS Appl. Mater. Interfaces 2015, 7, 10401−10406

Host-Guest Molecular Recognition. *Adv. Funct. Mater.* **2012**, *22*, 4742−4750.
(20) Ishihara, K.; Kobayashi, M.; Ishimaru, N.; Shinohara, I. Glucose Induced Permeation Control of Insulin through a Complex Membrane Consisting of Immobilized Glucose Oxidase and a Poly(amine). *Polym. J.* **1984**, *16*, 625−631.
(21) Chu, L. Y.; Li, Y.; Zhu, J. H.; Wang, H. D.; Liang, Y. J. Control of Pore Size and Permeability of a Glucose-Responsive Gating Membrane for Insulin Delivery. *J. Controlled Release* **2004**, *97*, 43−53.
(22) Kuroki, H.; Ito, T.; Ohashi, H.; Tamaki, T.; Yamaguchi, T. Biomolecule-Recognition Gating Membrane Using Biomolecular Cross-Linking and Polymer Phase Transition. *Anal. Chem.* **2011**, *83*, 9226−9229.
(23) Sugawara, Y.; Kuroki, H.; Tamaki, T.; Ohashi, H.; Ito, T.; Yamaguchi, T. Conversion of a Molecular Signal into Visual Color Based on the Permeation of Nanoparticles through a Biomolecule-Recognition Gating Membrane. *Anal. Methods* **2012**, *4*, 2635−2637.
(24) Jeon, G.; Yang, S. Y.; Kim, J. K. Functional Nanoporous Membranes for Drug Delivery. *J. Mater. Chem.* **2012**, *22*, 14814−14834.
(25) Martin, F.; Walczak, R.; Boiarski, A.; Cohen, M.; West, T.; Cosentino, C.; Shapiro, J.; Ferrari, M. Tailoring Width of Microfabricated Nanochannels to Solute Size Can Be Used to Control Diffusion Kinetics. *J. Controlled Release* **2005**, *102*, 123−133.
(26) Ling, X. Y.; Acikgoz, C.; Phang, I. Y.; Hempenius, M. A.; Reinhoudt, D. N.; Vancso, G. J.; Huskens, J. 3D Ordered Nanostructures Fabricated by Nanosphere Lithography Using an Organometallic Etch Mask. *Nanoscale* **2010**, *2*, 1455−1460.
(27) Montagne, F.; Blondiaux, N.; Bojko, A.; Pugin, R. Molecular Transport through Nanoporous Silicon Nitride Membranes Produced from Self-Assembling Block Copolymers. *Nanoscale* **2012**, *4*, 5880−5886.
(28) Tong, H. D.; Jansen, H. V.; Gadgil, V. J.; Bostan, C. G.; Berenschot, E.; van Rijn, C. J. M.; Elwenspoek, M. Silicon Nitride Nanosieve Membrane. *Nano Lett.* **2004**, *4*, 283−287.
(29) Sidorenko, A.; Tokarev, I.; Minko, S.; Stamm, M. Ordered Reactive Nanomembranes/Nanotemplates from Thin Films of Block Copolymer Supramolecular Assembly. *J. Am. Chem. Soc.* **2003**, *125*, 12211−12216.
(30) Yang, S. Y.; Ryu, I.; Kim, H. Y.; Kim, J. K.; Jang, S. K.; Russell, T. P. Nanoporous Membranes with Ultrahigh Selectivity and Flux for the Filtration of Viruses. *Adv. Mater.* **2006**, *18*, 709−712.
(31) Peinemann, K. V.; Abetz, V.; Simon, P. F. Asymmetric Superstructure Formed in a Block Copolymer via Phase Separation. *Nat. Mater.* **2007**, *6*, 992−996.
(32) Phillip, W. A.; O'Neill, B.; Rodwogin, M.; Hillmyer, M. A.; Cussler, E. L. Self-Assembled Block Copolymer Thin Films as Water Filtration Membranes. *ACS Appl. Mater. Interfaces* **2010**, *2*, 847−853.
(33) Nunes, S. P.; Behzad, A. R.; Hooghan, B.; Sougrat, R.; Karunakaran, M.; Pradeep, N.; Vainio, U.; Peinemann, K. V. Switchable pH-Responsive Polymeric Membranes Prepared via Block Copolymer Micelle Assembly. *ACS Nano* **2011**, *5*, 3516−3522.
(34) Phillip, W. A.; Dorin, R. M.; Werner, J.; Hoek, E. M.; Wiesner, U.; Elimelech, M. Tuning Structure and Properties of Graded Triblock Terpolymer-Based Mesoporous and Hybrid Films. *Nano Lett.* **2011**, *11*, 2892−2900.
(35) Liu, G.; Ding, J.; Hashimoto, T.; Kimishima, K.; Winnik, F. M.; Nigam, S. Thin Films with Densely, Regularly Packed Nanochannels: Preparation, Characterization, and Applications. *Chem. Mater.* **1999**, *11*, 2233−2240.
(36) Hu, H.; Liu, G. Miktoarm Star Copolymer Capsules Bearing pH-Responsive Nanochannels. *Macromolecules* **2014**, *47*, 5096−5103.
(37) Zhe-Xue, L.; Namboodiri, A.; Collinson, M. M. Self-Supporting Nanopore Membranes with Controlled Pore Size and Shape. *ACS Nano* **2008**, *2*, 993−999.
(38) Yan, F.; Ding, A.; Girones, M.; Lammertink, R. G. H.; Wessling, M.; Borger, L.; Vilsmeier, K.; Goedel, W. A. Hierarchically Structured Assembly of Polymer Microsieves, made by a Combination of Phase Separation Micromolding and Float-Casting. *Adv. Mater.* **2012**, *24*, 1551−1557.
(39) Yan, X.; Liu, G.; Dickey, M.; Willson, C. G. Preparation of Porous Polymer Membranes Using Nano- or Micro-Pillar Arrays as Templates. *Polymer* **2004**, *45*, 8469−8474.
(40) Zhang, Q.; Ghosh, S.; Samitsu, S.; Peng, X.; Ichinose, I. Ultrathin Freestanding Nanoporous Membranes Prepared from Polystyrene Nanoparticles. *J. Mater. Chem.* **2011**, *21*, 1684−1688.
(41) Peng, X.; Jin, J.; Nakamura, Y.; Ohno, T.; Ichinose, I. Ultrafast Permeation of Water through Protein-Based Membranes. *Nat. Nanotechnol.* **2009**, *4*, 353−357.
(42) Tokarev, I.; Orlov, M.; Minko, S. Responsive Polyelectrolyte Gel Membranes. *Adv. Mater.* **2006**, *18*, 2458−2460.
(43) Gopishetty, V.; Roiter, Y.; Tokarev, I.; Minko, S. Multiresponsive Biopolyelectrolyte Membrane. *Adv. Mater.* **2008**, *20*, 4588−4593.
(44) Tokarev, I.; Tokareva, I.; Minko, S. Gold-Nanoparticle-Enhanced Plasmonic Effects in a Responsive Polymer Gel. *Adv. Mater.* **2008**, *20*, 2730−2734.
(45) Gopishetty, V.; Tokarev, I.; Minko, S. Biocompatible Stimuli-Responsive Hydrogel Porous Membranes via Phase Separation of a Polyvinyl Alcohol and Na-Alginate Intermolecular Complex. *J. Mater. Chem.* **2012**, *22*, 19482−19487.
(46) Horcas, I.; Fernandez, R.; Gomez-Rodriguez, J. M.; Colchero, J.; Gomez-Herrero, J.; Baro, A. M. WSXM: A Software for Scanning Probe Microscopy and a Tool for Nanotechnology. *Rev. Sci. Instrum.* **2007**, *78*, 013705.
(47) Nečas, D.; Klapetek, P. Gwyddion: An Open-Source Software for SPM Data Analysis. *Cent. Eur. J. Phys.* **2012**, *10*, 181−188.
(48) Kim, J. W.; Kim, J. H.; Chung, S. J.; Chung, B. H. An Operationally Simple Colorimetric Assay of Hyaluronidase Activity Using Cationic Gold Nanoparticles. *Analyst* **2009**, *134*, 1291−1293.
(49) Qiu, X. Y.; Yu, H. Z.; Karunakaran, M.; Pradeep, N.; Nunes, S. P.; Peinemann, K. V. Selective Separation of Similarly Sized Proteins with Tunable Nanoporous Block Copolymer Membranes. *ACS Nano* **2013**, *7*, 768−776.
(50) Maki-Ontto, R.; de Moel, K.; de Odorico, W.; Ruokolainen, J.; Stamm, M.; ten Brinke, G.; Ikkala, O. "Hairy Tubes": Mesoporous Materials Containing Hollow Self-Organized Cylinders with Polymer Brushes at the Walls. *Adv. Mater.* **2001**, *13*, 117−121.
(51) Liu, J.; Hameed, N.; Guo, Q. Complexation and Eutectic Crystallization in Poly(2-vinyl pyridine)-*block*-poly(ε-caprolactone) and Pentadecylphenol Mixtures. *Eur. Polym. J.* **2010**, *46*, 2290−2299.
(52) Singamaneni, S.; Tsukruk, V. V. Buckling Instabilities in Periodic Composite Polymeric Materials. *Soft Matter* **2010**, *6*, 5681−5692.
(53) Kuroki, H.; Tokarev, I.; Nykypanchuk, D.; Zhulina, E.; Minko, S. Stimuli-Responsive Materials with Self-Healing Antifouling Surface via 3D Polymer Grafting. *Adv. Funct. Mater.* **2013**, *23*, 4593−4600.

DOI: 10.1021/acsami.5b01416
ACS Appl. Mater. Interfaces 2015, 7, 10401−10406